IEEE Photonics Journal
An IEEE Photonics Society Publication

Highly Birefringent, Low-Loss, and Near-Zero Flat Dispersion ENZ Based THz Photonic Crystal Fibers

Volume 12, Number 3, JUNE 2020

Md. Shahjalal Hossain
S. M. Abdur Razzak, ***Senior Member, IEEE***
Christos Markos, ***Member, OSA***
Nguyen Hoang Hai, ***Member, IEEE***
Md. Selim Habib, ***Senior Member, IEEE***
Md. Samiul Habib, ***Senior Member, IEEE***

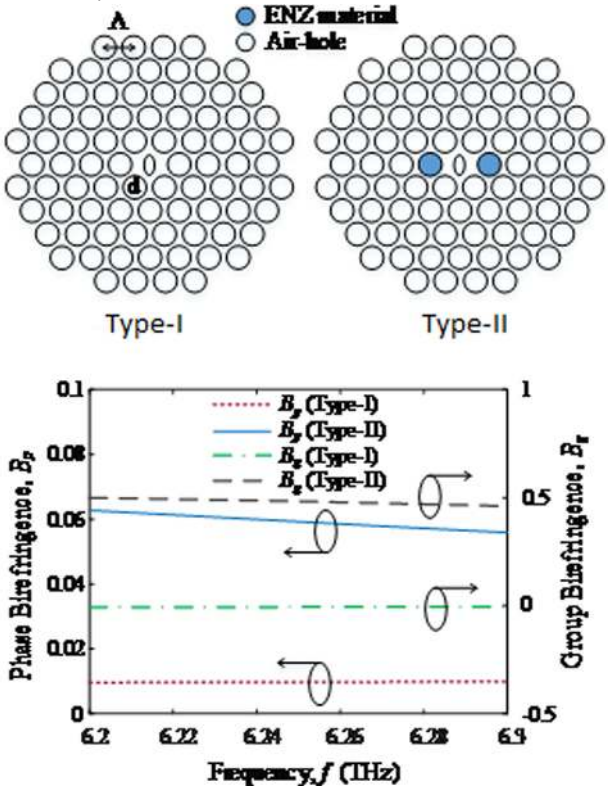

DOI: 10.1109/JPHOT.2020.2994108

Highly Birefringent, Low-Loss, and Near-Zero Flat Dispersion ENZ Based THz Photonic Crystal Fibers

Md. Shahjalal Hossain,[1] S. M. Abdur Razzak,[1] *Senior Member, IEEE*, Christos Markos,[2] *Member, OSA*, Nguyen Hoang Hai,[3] *Member, IEEE*, Md. Selim Habib,[4] *Senior Member, IEEE*, and Md. Samiul Habib,[1] *Senior Member, IEEE*

[1]Department of Electrical and Electronic Engineering, Rajshahi University of Engineering and Technology, Rajshahi 6204, Bangladesh
[2]Department of Photonics Engineering, Technical University of Denmark, 2800 Lyngby, Denmark
[3]School of Electronics and Telecommunication, Hanoi University of Science and Technology, Hanoi 100000, Vietnam
[4]Optoelectronics Research Group, Department of Electrical and Computer Engineering, Florida Polytechnic University, FL-33805 USA

DOI:10.1109/JPHOT.2020.2994108

Manuscript received April 10, 2020; revised May 4, 2020; accepted May 8, 2020. Date of publication May 14, 2020; date of current version June 29, 2020. Corresponding author: Md. Samiul Habib (e-mail: samiul.engr@ieee.org).

Abstract: In this paper, we present and compare two experimentally feasible photonic crystal fiber (PCF) designs (*Type-I* and *Type-II*) which ensure near-zero flattened dispersion with ultra-high phase and group birefringence at THz frequencies. Both structures are based on a subset of a triangular array of circular air-holes, which define the cladding of the PCF and a central elliptical air-hole which breaks the symmetry of the structure, thus introducing high levels of birefringence. Additionally, we investigate the possibility of further enhancing the birefringence properties of *Type-II* structure by selectively filling the air-holes with Potassium Chloride (KCl) as strong Epsilon-Near-Zero (ENZ) material. Our investigation reveals that significant enhancement of birefringence can be achieved than its original counterpart with birefringence to be as high as 0.0627 at 6.2 THz and near-zero flat dispersion of -0.54 ± 0.04 ps/THz/cm over the frequency range of 6.2−6.3 THz.

Index Terms: Photonic crystal fiber, ENZ material, dispersion, birefringence.

1. Introduction

Terahertz (THz) radiation is one of the significant parts of the electromagnetic spectrum, which bridges the two main technologically developed frequency bands, i.e., microwave and infrared frequencies and is roughly defined to lie between 0.1−10 THz. Over the last decade, this spectral region is widely used in many areas of science and industry, including airport security, sensing, material characterization, and is actively being researched for medical imaging and short-range wireless communications [1]. To date, a number of different techniques are being used to generate and detect THz waves [2], but most of the commercially available THz systems are still rely on

the free-space propagation. The major drawbacks of free-space propagation systems are that they severely affected by the unwanted absorption losses, and are difficult to integrate with other components towards monolithic devices.

Over the past few years, photonic crystal fibers (PCFs) are proven to be an excellent candidate as a waveguide and are being actively used in THz and optical regime. Contrary to conventional fibers, PCFs offer unique guiding properties, such as, endlessly single mode propagation, tailorable dispersion, high birefringence and good confinement ability [3]. Among various guiding properties, birefringence is one of the key factors in THz PCFs, and is highly desirable in many applications, e.g., in sensing, filtering, splitting, and polarization-based THz wave guiding [4]. Another important application of THz PCFs is in the data transmission purpose, where zero-flat dispersion is the primary requirements. The zero-flat dispersion prevents an optical signal from pulse spreading at the receiving end, consequently reducing the high bit error rates [5].

Over the past few decades, researchers have been proposed a variety of PCF structures with excellent guiding properties. For example, to achieve high birefringence, PCFs must be modeled in such a way that there is break of geometrical symmetry in the center core and/ or cladding regions. One of the common approaches to break the symmetry of PCFs is to introduce elliptical or rectangular air-holes in PCF. In 2012, Kim *et al.* proposed a PCF in which only elliptical air-holes are introduced in the core and cladding region. The structure ensures negative-flat dispersion of -156 ± 0.5 ps/nm/km in the telecommunication band with birefringence up to 10^{-2} [6]. Though the structure provides fairly high birefringence and flat dispersion, but the fabrication and practical feasibility of such a complex structure remains a crucial issue. Later, Habib *et al.* designed and numerically investigated a PCF having decagonal arrangement of circular air-holes at the cladding region and eight elliptical air-holes oriented at core region with reported birefringence of 0.0299 and negative-flat dispersion of -558.96 ps/nm/km [7]. Recently, a simple hexagonal PCF is numerically investigated in both THz and telecom band with reported birefringence of 0.105 and 0.07, respectively [4]. The PCF is filled with the ENZ material (KCL in THz band and AZO in telecom band) to achieve this result. Later, the same group proposes a new approach to attain a single-polarization-single-mode THz PCF by filling centre air-holes with the ENZ material [8]. However, a limited number of PCF structures have been proposed and analysed which exhibit high value of phase and group birefringence at a time [9], which we aim to overcome in this paper by introducing a realistic PCF structure.

In this paper, we propose a TOPAS-based PCF with experimentally feasible hexagonal shape suitable for the THz regime. The PCF constitutes with five air-hole rings in the cladding and only one elliptical air-hole at the central core region. The most congested air-holes in the cladding region ensure enhancement of the light confinement, resulting in a low total propagation loss. The center air-hole boosts the waveguide dispersion in conjunction to the material dispersion counterbalancing each other, thus maintaining the total dispersion in a "steady-state" [7] combined with the geometrical asymmetry which eventually leads to high birefringence. Then the two holes of the first ring are selectively infiltrated with ENZ material (KCl in our case) in order to further enhance the effective contrast between the *x*- and *y*-polarized modes.

2. Design Methodology

Fig. 1(a) represents the cross-sectional geometry of our proposed PCF configuration. The PCF has five air-hole rings arranged in a hexagonal fashion which defines the cladding region and an elliptical air-hole is located at the centre of the structure. The parameter *d* is the diameter of the circular holes, Λ is the pitch (distance between two adjacent air-hole) of the triangular lattice distribution, *a* and *b* are the diameters of the major and minor axis of the ellipse. The relation between the axes can be expressed as $b = \eta \times a$, where η represents the ellipticity. In our study, we use TOPAS as the main fiber material which has a fixed refractive index of 1.53 near 6.3 THz [4]. The optimized parameter configuration of the PCF to achieve near zero-flat dispersion, high birefringence and low loss has $\Lambda = 25\ \mu$m, $\mathrm{d}/\Lambda = 0.95$, $\mathrm{a} = 0.2\Lambda$, $\eta = 0.4$. In order to investigate the effect of ENZ, we consider two different cases of fiber structures, which we referred as, *Type-I*

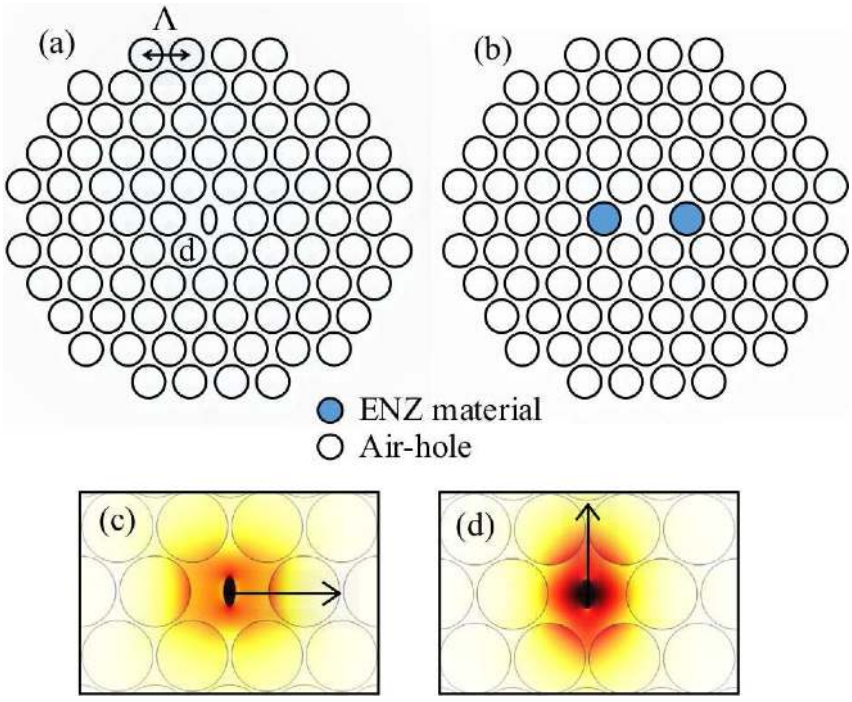

Fig. 1. Geometrical structure and air-hole arrangement of the proposed PCF. (a) *Type-I* PCF, (b) *Type-II* PCF (has ENZ material). Mode field distribution of (c) $x-$polarized and (d) $y-$polarized wave for *Type-II* PCF.

and *Type-II*, respectively. In *Type-I* structure, the PCF constitutes of only air-holes (without ENZ material) and represents the conventional type of PCF, in which high birefringence is obtained by simply introducing geometrical asymmetry with single elliptical air-hole at the core region. In contrast, two air-holes of the first ring of *Type-II* PCF are selectively filled with ENZ material. The latter design uses KCl as the ENZ material, which has been found promising material for the frequency range of 6.2–6.3 THz [10]. The fundamental mode field distribution of x-polarized and y-polarized wave is shown in Fig. 1(c) and (d). Here, we consider the field distribution only for *Type-II* PCF and is calculated at 6.3 THz. From the field distribution, it is noticed that the fundamental modes are well confined in the centre core region, as expected because of higher index contrast at the core region compared with the outer cladding region.

3. Numerical Results and Discussion

The guiding properties of the proposed PCFs is calculated using the state-of-the-art finite-element based COMSOL software. Perfectly-matched layer boundary conditions were used to accurately calculate the confinement loss. The main guiding parameters, which define the performance of a PCF are phase and group birefringence, waveguide dispersion and effective material loss (EML) and are defined mathematically as [9], [11].

$$B_p = |n_x - n_y|, \tag{1}$$

$$B_g = B_p - \lambda \frac{dB_p}{d\lambda}, \tag{2}$$

$$\beta_2 = \frac{2}{c}\frac{dn_{\text{eff}}}{d\omega} + \frac{\omega}{c}\frac{d^2 n_{\text{eff}}}{d\omega^2}, \tag{3}$$

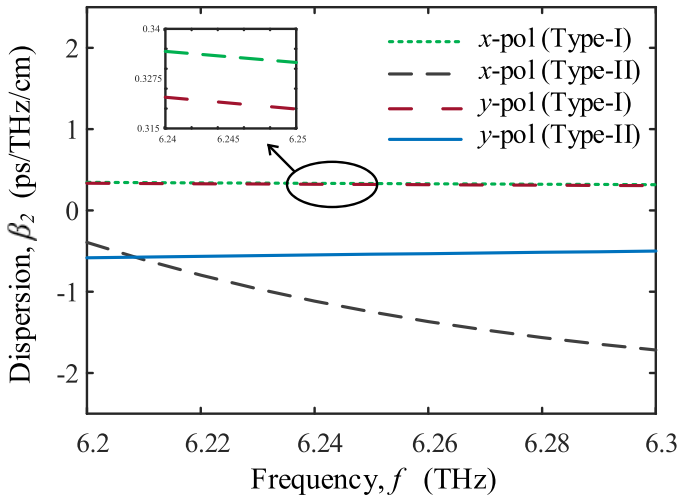

Fig. 2. Dispersion as a function of frequency for both *Type-I* and *Type-II* PCF.

$$\alpha_{\text{eff}} = \sqrt{\frac{\epsilon_0}{\mu_0}} \frac{\int n_{\text{mat}} \alpha_{\text{mat}} |E|^2}{2 \int S_z dA}, \tag{4}$$

Where, B_p, B_g, β_2 and α_{eff} are the phase birefringence, group birefringence, waveguide dispersion, confinement loss and EML, respectively. n_{eff} is the real part of effective index, n_x and n_y are the effective index for $x-$ and $y-$ polarized mode, respectively, ε_0 and μ_0 is the permittivity and permeability in vacuum, α_{mat} is the bulk material absorption loss, n_{mat} is the refractive index of the background material, E is the electric field of fundamental mode, A is effective modal area and S_z is the Poynting vector along the z direction.

In this study, we provide a direct comparison of the two PCFs and clarify which one is better for the THz regime. Fig. 2 shows the near zero-flat dispersion behavior of the two proposed designs. *Type-I* exhibits the absolute dispersion variation of 0.028 ps/THz/cm for $x-$polarization and 0.029 ps/THz/cm for $y-$polarization. On the other hand, *Type-II* shows the absolute dispersion variation 1.32 ps/THz/cm for $x-$polarization and 0.08 ps/THz/cm for $y-$polarization. We found very high phase and group birefringence of 0.0627 and 0.4995 at 6.2 THz, respectively for *Type-II* PCF, which is shown in Fig. 3. For *Type-II* PCF, the minimum EML of 0.116 cm^{-1} for $x-$and 0.09 cm^{-1} for $y-$polarization is found at 6.3 THz as shown in Fig. 4.

We have found extremely high birefringence, comparatively low EML and near zero-flat dispersion using ENZ material. *Type-II* PCF exhibits appreciable result for $y-$polarization and so, in the following sections, we will focus on *Type-II* PCF for $y-$polarization. Parameter sweep have been used for analyzing the effects of d_1 (diameter of the first rings holes), η and Λ on guiding properties of the *Type-II* PCF.

3.1 Effect of Diameter d_1

In our previous work, we show that the diameter of the first rings holes, d_1 not only maintain the near zero-flat dispersion but also changes the slope of the dispersion curve [7]. The parameter sweep for d_1 is performed by varying it from 0.85Λ to 0.95Λ to investigate the optimum frequency of operation. The variation of dispersion and birefrigence due to the change of d_1 is shown in Figs. 5 and 6. The variation of d_1 results in change of the slope of the dispersion curves, as expected, but we found almost flat dispersion for varying normalized d_1 from 0.85 to 0.95. As two of the holes are selectively filled with *ENZ* material, the reduction of the normalized d_1 means the reduction of the amount of the ENZ material, leads to lower birefringence due to the reduced effective index contrast.

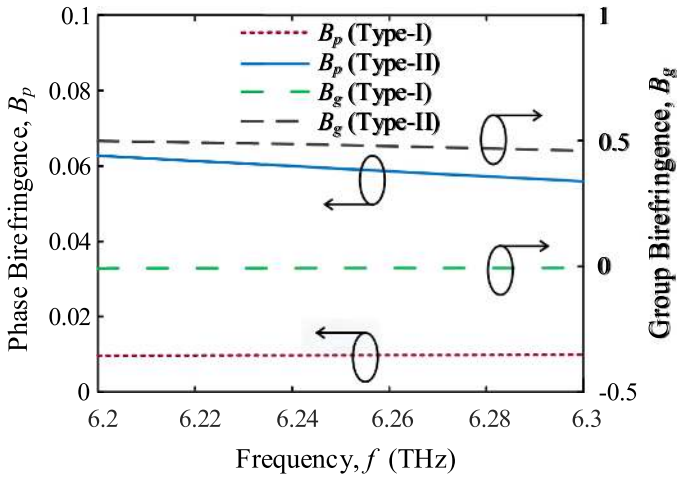

Fig. 3. Phase and group birefringence as a function of frequency for both *Type-I* and *Type-II* PCF.

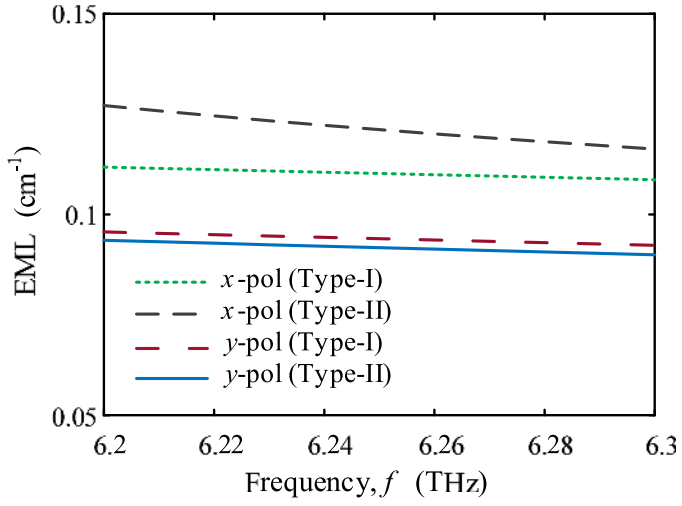

Fig. 4. EML as a function of frequency for both *Type-I* and *Type-II* PCF.

3.2 Effect of Ellipticity η

Ellipticity, η is another important geometrical parameter which plays a crucial role in order to increase the birefringence and the zero-flat dispersion. From Fig. 7, it is clearly seen that the dispersion for $y-$polarization is almost unaffected with varying η from 0.5 to 0.3. However, a significant result emerges on birefringence according to the change of η. Fig. 8 clarifies that the attainment of the higher birefringence is possible by reducing the value of η because reducing the aspect ratio asymmetry is further enhanced. However, it should be noted that the thinner the ellipse is the more challenging the fiber fabrication becomes.

3.3 Effect of Pitch Λ

The change of the parameter Λ affects directly the dispersion characteristics of the PCF. The variation of Λ shifts the dispersion level keeping the slope unchanged [7], [12]. During this investigation, Λ was varied from 25 μm to 30 μm. Fig. 9 shows how the dispersion curve only shifts their level by changing Λ. However, on the other hand, the birefringence for the same variation of

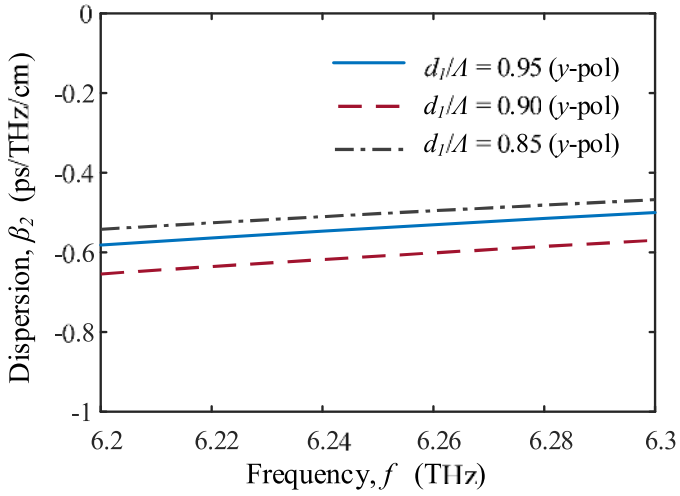

Fig. 5. Dispersion as a function of frequency for the variation of d_1.

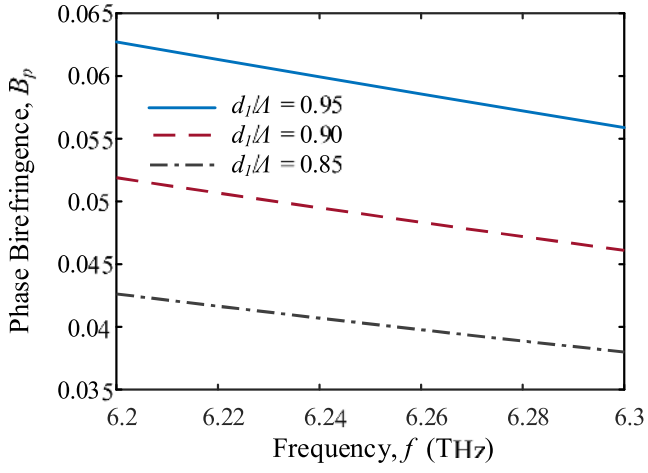

Fig. 6. Birefringence as a function of frequency for the variation of d_1.

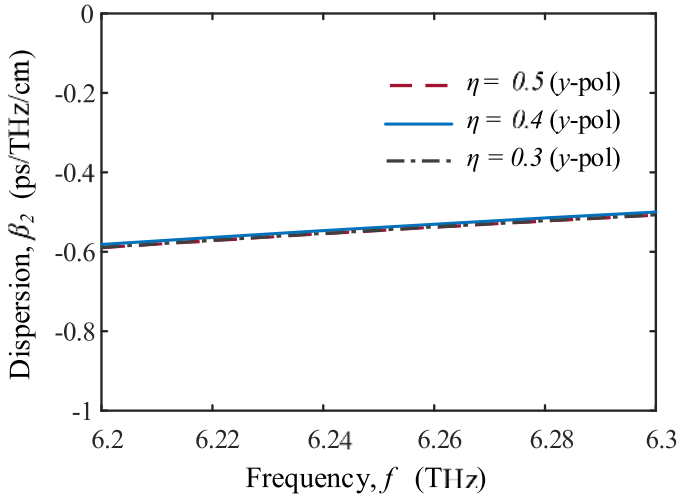

Fig. 7. Dispersion as a function of frequency for the variation of η.

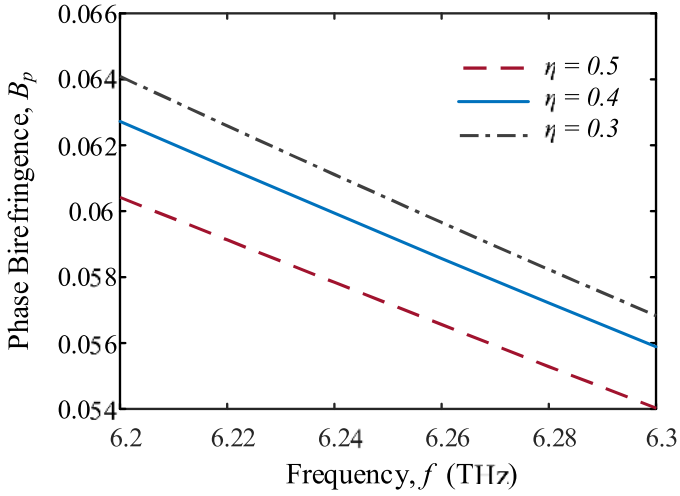

Fig. 8. Birefringence as a function of frequency for the variation of η.

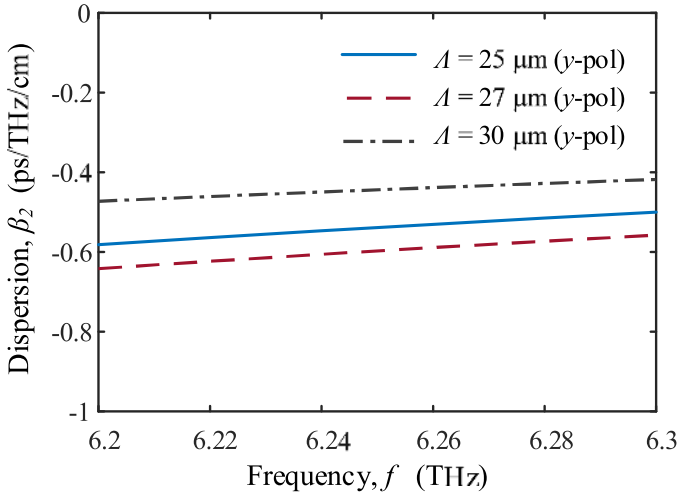

Fig. 9. Dispersion as a function of frequency for the variation of Λ.

Λ, shown in Fig. 10, reveals that birefringence is decreasing with the reduction of Λ, which is expected.

In this work, we presented and directly compared two different fiber designs towards novel fiber devices with optimized guiding properties. Considering the behavior of the PCF by varying different structural parameters i.e., d_1, η, and Λ, the PCF properties are discussed. Our PCF structure relies on circular air-holes of same diameter and has only one elliptical air-hole at the centre, whereas in [4] two dissimilar diameter of air-holes were used, making the structure extremely challenging to fabricate with the most common fiber drawing technique. Since elliptical air-hole has been possible to fabricate in the laboratory, our proposed PCF having only one elliptical air-hole seems experimentally feasible and realistic [13], [14]. It is important to note that methods of integrating single metallic wires and also metamaterials into the complex fiber structures have been practically implemented in [15], [16]. Since our proposed Type-II PCF structure contains selectively filled air-holes with naturally occurring ENZ material, the implantation of ENZ material into the fiber air-holes is possible using the well-established fabrication techniques, e.g., direct thermal drawing [15], pressure-assisted melt filling technique [17], or chemical deposition technique [18].

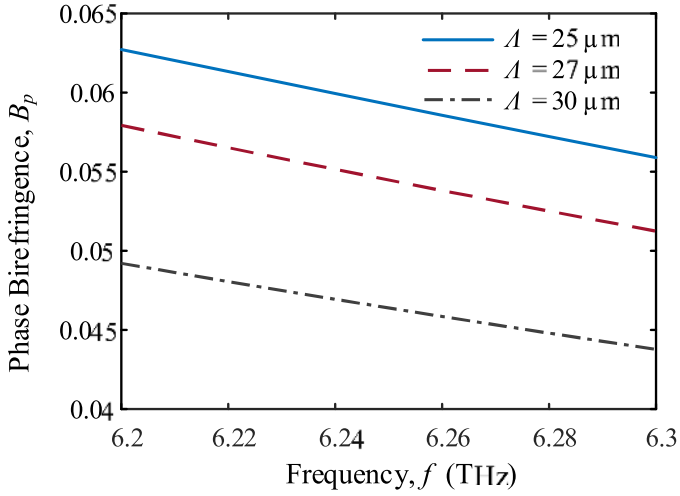

Fig. 10. Birefringence as a function of frequency for the variation of Λ.

We believe that our PCF structure can be practically implemented using the pressure-assisted melt filling technique to implant the bulk form of KCl into appropriate air-holes without any major complications [4].

4. Conclusion

In this paper, a relatively new type of hexagonal PCF has been demonstrated which has high phase and group birefringence, near zero-flat dispersion and low loss over the frequency range of 6.2–6.3 THz. By introducing asymmetry in the geometrical structure and material distribution, birefringence can be further enhanced. In particular, high birefringence can be achieved by developing index contrast at the core region by selectively filling the fiber with the ENZ material. Our PCF exhibits near zero-flat dispersion of -1.05 ± 0.66 ps/THz/cm for $x-$polarization and -0.54 ± 0.04 ps/THz/cm for $y-$polarization over the range $6.2 - 6.3$ THz and EML of 0.116 cm^{-1} for $x-$ and 0.09 cm^{-1} for $y-$polarization at 6.3 THz. Extremely high phase and group birefringence of 0.0627 and 0.4995 obtained, respectively. Its guiding properties remain less unaffected when parameter sweep is applied. The proposed structure is relatively easy to fabricate as it is based on circular air-holes of same diameter at the cladding and only one elliptical air-hole at the core region. So, it can be a potential solution towards development of fiber devices for the THz regime.

Acknowledgment

The authors would like to thank the anonymous reviewers for their valuable suggestions.

References

[1] A. Redo-Sanchez and X.-C. Zhang, "Terahertz science and technology trends," *IEEE J. Sel. Top. Quantum Electron.*, vol. 14, no. 2, pp. 260–269, Mar./Apr. 2008.
[2] W. L. Chan, J. Deibel, and D. M. Mittleman, "Imaging with terahertz radiation," *Rep. Prog. Phys.*, vol. 70, no. 8, p. 1325, 2007.
[3] P. Russell, "Photonic crystal fibers," *Science*, vol. 299, no. 5605, pp. 358–362, 2003.
[4] T. Yang, C. Ding, R. W. Ziolkowski, and Y. J. Guo, "Circular hole ENZ photonic crystal fibers exhibit high birefringence," *Opt. Express*, vol. 26, no. 13, pp. 17 264–17 278, 2018.
[5] D. Tee, M. A. Bakar, N. Tamchek, and F. M. Adikan, "Photonic crystal fiber in photonic crystal fiber for residual dispersion compensation over E + C + L + U wavelength bands," *IEEE Photon. J.*, vol. 5, no. 3, Jun. 2013, Art. no. 7200607.

[6] S. E. Kim, B. H. Kim, C. G. Lee, S. Lee, K. Oh, and C.-S. Kee, "Elliptical defected core photonic crystal fiber with high birefringence and negative flattened dispersion," *Opt. Express*, vol. 20, no. 2, pp. 1385–1391, 2012.
[7] M. S. Habib and E. Khandker, "Highly birefringent photonic crystal fiber with ultra-flattened negative dispersion over S+C+ L+ U bands," *Appl. Opt*, vol. 54, no. 10, pp. 2786–2789, 2015.
[8] T. Yang, C. Ding, R. W. Ziolkowski, and Y. J. Guo, "A terahertz (THz) single-polarization-single-mode (SPSM) photonic crystal fiber (PCF)," *Materials*, vol. 12, no. 15, pp. 2442–2456, 2019.
[9] M. S. Alam, K. Saitoh, and M. Koshiba, "High group birefringence in air-core photonic bandgap fibers," *Opt. Lett.*, vol. 30, no. 8, pp. 824–826, 2005.
[10] A. Reyes-Coronado *et al.*, "Self-organization approach for THz polaritonic metamaterials," *Opt. Express*, vol. 20, no. 13, pp. 14 663–14 682, 2012.
[11] G. Hasanuzzaman, M. S. Habib, S. A. Razzak, M. A. Hossain, and Y. Namihira, "Low loss single-mode porous-core kagome photonic crystal fiber for THz wave guidance," *J. Lightw. Technol.*, vol. 33, no. 19, pp. 4027–4031, Oct. 2015.
[12] M. S. Habib, M. S. Habib, M. Hasan, and S. Razzak, "A single mode ultra flat high negative residual dispersion compensating photonic crystal fiber," *Opt. Fiber Technol.*, vol. 20, no. 4, pp. 328–332, 2014.
[13] N. A. Issa, M. A. van Eijkelenborg, M. Fellew, F. Cox, G. Henry, and M. C. Large, "Fabrication and study of microstructured optical fibers with elliptical holes," *Opt. Lett.*, vol. 29, no. 12, pp. 1336–1338, 2004.
[14] H. Ebendorff-Heidepriem and T. M. Monro, "Extrusion of complex preforms for microstructured optical fibers," *Opt. Express*, vol. 15, no. 23, pp. 15 086–15 092, 2007.
[15] J. Hou, D. Bird, A. George, S. Maier, B. T. Kuhlmey, and J. Knight, "Metallic mode confinement in microstructured fibres," *Opt. Express*, vol. 16, no. 9, pp. 5983–5990, 2008.
[16] A. Tuniz, R. Lwin, A. Argyros, S. C. Fleming, and B. T. Kuhlmey, "Fabricating metamaterials using the fiber drawing method," *J. Vis. Exp.*, vol. 68, no. 68, pp. e4299–4309, 2012.
[17] H. Lee *et al.*, "Pressure-assisted melt-filling and optical characterization of au nano-wires in microstructured fibers," *Opt. Express*, vol. 19, no. 13, pp. 12 180–12 189, 2011.
[18] R. He *et al.*, "Integration of gigahertz-bandwidth semiconductor devices inside microstructured optical fibres," *Nature Photon.*, vol. 6, no. 3, pp. 174–179, 2012.